Cirrus clouds and deep convection in the tropics: Insights from CALIPSO and CloudSat

Kenneth Sassen,[1] Zhien Wang,[2] and Dong Liu[2]

[1] Using a 2-year data set of combined lidar and cloud radar measurements from the Cloud-Aerosol Lidar and Infrared Pathfinder Satellite Observations (CALIPSO) and CloudSat satellites, the occurrence of tropical cirrus and deep convective clouds is studied. The cloud identification algorithm takes advantage of the ability of the radar to probe deep precipitating clouds and of the lidar to sample even subvisual cirrus clouds. Examined are the frequency of occurrence and the geographical distribution of these clouds, and their apparent interconnections. There is a strong apparent diurnal variability in tropical cirrus mainly over land, with significantly more cirrus detected at night compared to day, but no clear diurnal pattern in deep convective activity. CALIPSO daylight signal noise effects do not appear to be not responsible for the diurnal cirrus pattern, because high, thin tropopause transitional layer (TTL) cirrus do not show a clear diurnal effect. Stratifying the global results by estimated visible cloud optical depth τ, we find that most of the planet's subvisual ($\tau < {\sim}0.03$) cirrus clouds occur in the tropics and are more frequent at night and over ocean; thin (${\sim}0.03 < \tau < {\sim}0.3$) cirrus have their highest global frequencies over equatorial landmasses and in the west Pacific region, and are also more frequent at night but occur mainly over land; and opaque (${\sim}0.3 < \tau < {\sim}3.0$) cirrus are spread globally and tend to occur during the day over ocean. Although it is unknown which of the several proposed cirrus cloud formation mechanisms are key in the tropics, the close association of cirrus with convective clouds implies that tropical cirrus are linked to deep convective activity, with the likely exception of TTL cirrus clouds.

1. Introduction

[2] The classic images of the Earth from space are likely to show cloud swirls associated with midlatitude storms, expanses of oceanic stratus cloud decks, and a consistently dominant feature: the highly reflective band of clouds situated in the equatorial belt virtually around the globe. This region of the Earth that receives the most heat from the Sun must also dissipate it through ocean and air currents, evaporation, and reradiation to outer space in the infrared spectral region. Indeed, the flux of heat from the tropics poleward is the engine that drives global weather, so understanding the tropics is key to predicting weather and climate. Cloud formation here is of key importance because it can strongly modulate the atmospheric heat balance through latent heating and significantly redirect radiation through water phase changes.

[3] Unfortunately, the vertical structure of tropical clouds is complex and not well understood despite its global importance. Deep cumulus convection with rainfall seems common and can dominate vast regions, such as seasonal monsoon flows into coastal areas and the yearly north-south migrating Intertropical Convergence Zone (ITCZ). Where land occurs lay the jungles of the Amazon Basin, central Africa, and the Micronesian island chain. When viewed from space, the high storm tops and the spreading cirrus anvils ejected from them are readily evident. Convective cloud towers and any associated regions of steady rain are likely to occupy relatively small areas compared to the cirrus cloud shields that result from anvil wind shear and horizontal transport processes. By cirrus clouds we mean those ice clouds of the upper troposphere that would be identified visually as such by a trained surface weather observer, which excludes optically denser clouds such as altostratus. Research has shown that cirrus clouds are gray body emitters (infrared emittances $< {\sim}0.85$) and semitransparent to sunlight (visible optical depth $\tau < {\sim}3.0$), and thus much spreading of the dense cumulonimbus cloud tops is required to qualify them as true cirrus, with their much greater areal distribution than the convective cores [*Sassen*, 2002].

---

[1]Geophysical Institute, University of Alaska Fairbanks, Fairbanks, Alaska, USA.
[2]Atmospheric Science Department, University of Wyoming, Laramie, Wyoming, USA.

[4] Tropical cirrus clouds also depend on deep convection because the clouds are themselves a sink for water vapor in the upper troposphere/lower stratosphere through ice particle growth and fallout [*Jensen et al.*, 1996; *Rosenfield et al.*, 1998], and this vapor needs to be replenished. Convective clouds do this directly through detrainment and mixing with ambient air, and may also aid in cirrus formation in the tropopause transition layer (TTL) through convective cloud top radiative cooling or causing the upward movement and expansion of air forced by wind over cumulus towers [*Garrett et al.*, 2006]. The apparently extensive nature of thin tropical cirrus layers has been pointed out using satellites [*Prabhakara et al.*, 1993; *Wang et al.*, 1996; *Bourassa et al.*, 2005], previous spaceborne lidars [*Winker and Trepte*, 1998; *Dessler et al.*, 2006], and ground-based remote sensing [*Platt et al.*, 1998, 2002; *Comstock et al.*, 2002; *Cadet et al.*, 2003; *Iwasaki et al.*, 2004]. Limited aircraft studies of high tropical cirrus have also been made [*Heymsfield*, 1986; *McFarquhar et al.*, 2000]. Once formed in the vicinity of active convection, however, the cirrus must be maintained over time by radiative or dynamical processes that are unrelated to the initial detrainment of ice and the local cooling effects of towers. It has been speculated that synoptic-scale ascent and vertically propagating Kelvin or gravity waves, often themselves initiated by organized convection, could be contributing to cirrus formation in areas distant from deep tropical convection [*Boehm and Verlinde*, 2000]. Nonetheless, these cold trap cirrus [*Sassen*, 2002], which form at the coldest tropospheric temperatures encountered on Earth and tend to be optically thin or subvisual, may still depend on humidification via tropical thunderstorms.

[5] According to the recent spaceborne (i.e., CloudSat and CALIPSO) active remote sensing results given by *Sassen et al.* [2008], the amounts of cirrus clouds in the tropical (say up to ± 15° latitude from the equator) and tropical plus subtropical (±30° latitude) zonal belts are a significant proportion of the planets' cirrus cloud cover. The total 1-year global mean cirrus cloud frequency was reported at 16.7%, but about 35% of this cirrus coverage occurred within ±15° latitude and 56% within ±30° latitude of the equator. This amount of cirrus is clearly significant, and yet the basic cloud formation processes, which control in fundamental ways the cirrus cloud microphysical/radiative properties, are not well comprehended. Cirrus clouds are normally regarded as thermal blankets (i.e., greenhouse contributors) that absorb and trap part of the radiation emitted by the warm surface of the Earth, but many scenarios are possible in the vertically complex cloud systems and extremely cold conditions atop the tropical troposphere.

[6] Much of what we know regarding the importance of deep convection on the formation of tropical cirrus (both directly anvil generated and TTL level) has come, for example, from ground-based or airborne lidar case studies [*Platt et al.*, 1998, 2002; *Sassen et al.*, 2000] and passive satellite measurements combined with isentropic back trajectories to locate cirrus sources [*Mace et al.*, 2006]. Drawbacks with these attempts, however, have to do with the quite limited field experiment locations and campaign periods, and the well-known limitations in inferring three-dimensional cloud properties using only passive remote

sensors on satellites. Now, for the first time, active remote sensors in Earth orbit can be brought to bear on this problem. In April 2006 were launched the CloudSat Cloud Profiling Radar (CPR) and the Cloud-Aerosol Lidar and Infrared Pathfinder Satellite Observations (CALIPSO) Cloud-Aerosol Lidar with Orthogonal Polarization (CALIOP) payloads as part of the new concept of the A-train of formation-flying satellites [*Stephens et al.*, 2002; *Winker et al.*, 2007].

[7] In this study we use the combined 2-year data set (beginning 15 June 2006) from CloudSat and CALIPSO, each with their own advantages and limitations for cloud research, to better understand the connections between deep tropical convection and cirrus clouds. CloudSat radar measurements are particularly well suited to identifying the former, while CALIPSO lidar the latter. After briefly describing the cloud detection algorithm, the mean frequencies of tropical cirrus and deep convective clouds are given according to geographic location, height, night versus day, and season. Then the issue of the apparent diurnal variations in cirrus cloud frequency is addressed with the help of case studies of regional cirrus properties. Also examined are the basic characteristics of tropical cirrus clouds and how their optical and height properties differ from their counterparts at higher latitudes. We conclude with a discussion of the indicated connections between tropical cirrus clouds and the presence of deep convection.

2. CloudSat/CALIPSO Data Analysis

[8] It is well established that lidars are better able to detect cold, optically thin cirrus clouds than even the most sensitive millimeter-wave cloud radars because the cirrus ice crystal backscattering with radar varies according to the particle diameter D^6 Rayleigh law, whereas lidars are able to better sense the entire particle spectra according to the D^2 geometrical optics law. Thus lidars can detect high-altitude tropical cirrus clouds containing relatively minute ice particles that cloud radars cannot, and in general the top heights of cirrus clouds are underestimated by radar [e.g., *Comstock et al.*, 2002]. However, the opposite is true when it comes to probing deep convective clouds, for lidar pulses can be attenuated away after penetration depths of as little as a few hundred meters in dense ice and water clouds: the great sensitivity of lidar to small cloud particles comes at a cost. Attenuation does also impact CPR probing in deep convective clouds to some degree, but this can be used to advantage in developing algorithms for identifying deep convection by CloudSat. Rainfall, and to a lesser extent snowfall, can generate noticeable millimeter-wave radar extinction, which can lead to apparent radar bright bands in the melting region and cause the return from the surface of the Earth to be absent, or diminished in strength, due to heavy extinction in rain [*Matrosov*, 2007; *Sassen et al.*, 2007]. Thus the lidar/radar sensors in the A-train are in principle well suited for studying both thin cirrus and deep convective clouds.

[9] The algorithms we have developed for identifying both cirrus and deep convective clouds (DCC) are based on standard Level 2 CloudSat and hybrid CloudSat plus CALIPSO science team activities. For DCC like precipitating cumulonimbus or cumulus congestus, the CPR reflec-

tivity profiles alone are sufficient for their identification using the CloudSat Level 2 Cloud Scenario Classification Product Process Description and Interface Control Document, Version 5.0 (available from http://cloudsat.cira.colostate.edu/ dataICDlist.php?go=list&path=/2B-CLDCLASS). This algorithm requires a sufficient radar echo depth (>6.0 km) and strength (>10 dBZ) along with the presence of low-level precipitation, and tests for horizontal extent and temperature structure, to identify a radar return feature as a DCC. A previous comparison of the CloudSat DCC algorithm results with zonal-averaged surface and satellite findings shows that all the results are similar in the tropics, except surface reports of DCC over ocean exceeded the other results [*Sassen and Wang*, 2008].

[10] For cirrus cloud identification it is mainly CALIOP data that is relied on, although CPR information is considered in defining the cloud base heights in optically thick cirrus. So, we begin with the combined cloud mask algorithm, the 2B-GEOPROF-LIDAR version 002 (available from http://www.cloudsat.cira.colostate.edu/dataICDlist. php?go=list&path=/2B-GEOPROF-LIDAR), and then apply tests to determine if the high-altitude clouds identified are true cirrus clouds. In view of the previous discussion and as described in detail by *Sassen et al.* [2008], it is determined whether the cloud layer is transparent to lidar probing (i.e., $\tau < \sim 3.0-4.0$) by searching for the presence of a lower cloud layer or the surface return, and then a temperature test is applied: the cirrus cloud top must be $<-40°C$ based on climatological cirrus cloud findings [*Sassen*, 2002]. On the other hand, no a priori maximum or minimum cloud height criteria for identifying cirrus come into play in the tropics [see *Sassen et al.*, 2008].

[11] To estimate the cirrus cloud visible optical depth τ from the CALIPO data, we use the backward Fernald method with a mean effective lidar (extinction-to-backscatter) ratio of 20 sr. According to ground-based lidar studies, the lidar ratio is dependent on cirrus cloud optical depth as well as cloud temperature [*Platt et al.*, 1998; *Chen et al.*, 2002], but an effective lidar ratio (accounting for the contribution from multiple scattering) of 20 sr represents an acceptable mean value for our purposes. On an individual case basis, errors in τ arising from using this simple approach could be as high as a factor of $2-3$, but note that we calculate τ only to put the cirrus into the broad categories of subvisual ($\tau < \sim 0.03$), thin ($\sim 0.03 < \tau < \sim 0.3$), and opaque ($\sim 0.3 < \tau < \sim 3.0$) cirrus clouds [*Sassen and Cho*, 1992].

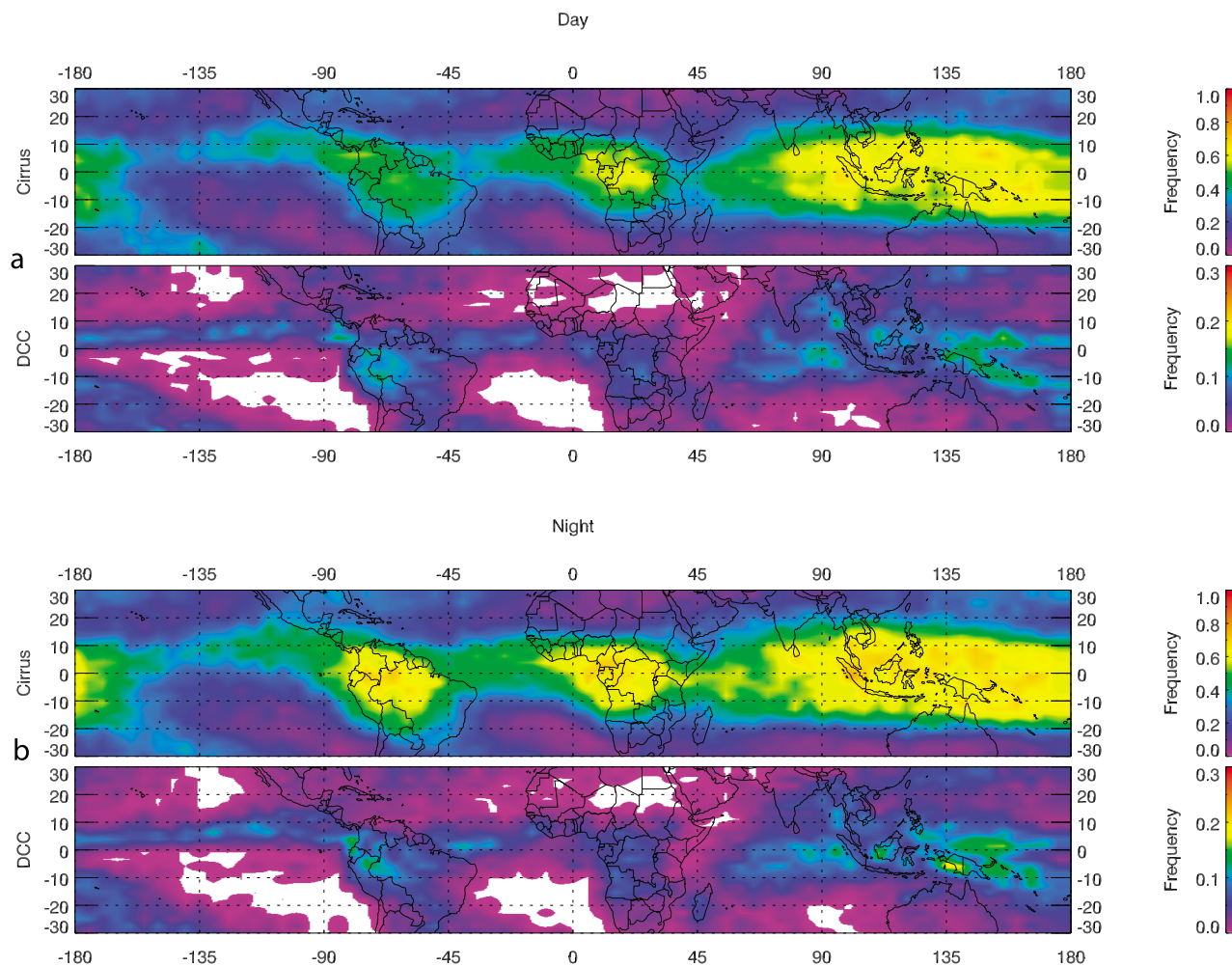## 3. Tropical Deep Convection and Cirrus Frequencies

[12] Because the A-train satellite formation flies in a Sun-synchronous 705 km orbit, with repeated 0130 and 1330 local mean times for crossing the equator [*Stephens et al.*, 2002], CloudSat and CALIPSO measurement times worldwide are in the early afternoon and just after midnight. Thus, the measurements are divided into day and night data sets where some measure of diurnal variability may be preserved. Diurnal cloud variations will be examined in more detail in section 4 with total night plus day average cloud frequencies and night minus day frequencies to highlight differences, but here we will show the mean day and night data displayed separately within the $\pm 23.4°$

equatorial belt (but extending to $\pm 30°$) for each $5.0°$ longitude by $2.5°$ latitude grid box used for averaging the 2-year data set.

[13] Figures 1a and 1b show the cirrus and DCC frequencies for night and day, respectively. As in our earlier 1-year climatological study [*Sassen et al.*, 2008], it is clear that the maximum cirrus amounts occur over the western Pacific warm pool area (up to $\sim 70\%$ coverage), the equatorial sections of western Africa and South America, and to a somewhat lesser extent the linear feature associated with the Inter-Tropical Convergence Zone that tends to tie these areas together. With the exception of the rather narrow ITCZ, most cirrus and DCC occur over or adjacent to landmasses and island chains, with the exception of the central Pacific Ocean area. In the subtropics many areas have little cirrus occurrence apparently due to the descending motions in the Hadley cell circulation and the almost complete lack of deep convection, at least at those local times probed by the A-train satellites. Comparing the night and day cirrus amounts reveals that appreciably more cirrus are identified by our algorithm during night measurements, but the overall patterns are quite similar.

[14] It is clear that the geographical distribution pattern of DCC is quite similar to that of the cirrus cloud coverage. Thus, the general occurrence of cirrus clouds is well correlated with the locations of deep convective clouds in the tropical region, although obviously not on a one-to-one relationship because of the limited areas occupied by convective cloud tops relative to anvil spreading, for example. Cirrus cloud frequencies are typically lowest (<10%) where deep convection is essentially absent. This implies that the formation mechanisms of the two cloud types are in some way related, either directly through anvil spreading, or indirectly. The indirect connections may involve cirrus occurrence changes due to the radiative effects from lower, colder cloud tops versus the warm surface, TTL humidification via penetrating turrets, regional updrafts via a pileus cloud analog, and gravity waves spawned by convection. Some regional exceptions to the cirrus/DCC linkage occur, such as off the coasts of Ecuador and equatorial western Africa, where deep convection ends along the coastlines and what appears to be anvil blow-off continues to the northwest over ocean.

[15] To examine these connections in more detail, given in Figures 2a and 2b are the same 2-year average night and day results broken into seasons. At this level, details like the Northern Hemisphere summer monsoonal maximum in deep convection, the highest of any DCC amounts, and cirrus in the Bay of Bengal are apparent, with indications of a day/night shift in the location of the greatest DCC amount at this location. Also in JJA, an anomaly exists nearby in the Indian Ocean just off the east coast of Africa, where a cirrus maximum occurs without much indication of DCC. The conditions in boreal winter and spring are dominated by the southward migration of the ITCZ and the explosion of cirrus and deep convection over northern South America, equatorial Africa, and the western and central Pacific Ocean area. A small DCC and cirrus cloud maximum is also found in DJF over the island of Madagascar, indicating the importance of land to cloud formation [see also *Mace et al.*, 2006]. Cirrus associated with the ITCZ are most pronounced across the mid-Pacific and Atlantic oceans during

Figure 1. Latitude versus longitude display comparing mean cirrus cloud (Cirrus) and deep convective cloud (DCC) frequency of occurrence in the tropical/subtropical (±30°) belt derived from CALIPSO and CloudSat data for (a) day (~1330 local time) measurements and (b) night (~0130 local time). Unless otherwise stated, all plots given here represent a 2-year average of data over 5.0° longitude by 2.5° latitude boxes.

MAM and SON. Particularly over landmasses and their downwind coasts, the cirrus appear to have a strong diurnal variation, although the DCC over land are apparently not much different from day to night (see below).

4. Indicated Diurnal Variability

[16] The above discussion, as well as our previous CloudSat/CALIPSO cirrus research [*Sassen et al.*, 2008], indicates the presence of a diurnal tide in cirrus cloud occurrence frequencies in the tropics, with nighttime cirrus showing a clear dominance in cirrus coverage. But are there other explanations for this apparent pattern? It was concluded by *Sassen et al.* [2008] that daylight signal noise effects on CALIPSO lidar cirrus cloud detection versus night appeared responsible for on the order of a 2% loss of cirrus globally, but there is a higher potential for sampling errors in the tropics if optically thin or subvisual cirrus congregate there (see section 7). Moreover, because of the high Sun angles during tropical daytime overpasses, background lidar signals are uniquely high due to the peak

in the solar scattering phase function of ice crystals near 180°, as well as the opportunity for the signals to be influenced by ocean solar glint effects. In this section we begin to address this issue with the presentation of the mean day plus night frequencies and the mean night minus day differences for cirrus and DCC, as shown in Figure 3. In section 5 are examined more detailed day versus night case studies of regional cirrus properties, so as not to over-average the data in space and time.

[17] The model usually applied to the diurnal cycle of tropical thunderstorms involves a peak occurrence over land that occurs in the late afternoon or early evening, essentially due to the effects of surface solar heating and the rise of the humid boundary layer, while over ocean an early morning peak is indicated [e.g., *Gray and Jacobson*, 1977; *Yang and Slingo*, 2001; *Liu and Zipser*, 2008]. In essence, this cycle is controlled by dynamical features related to the balance between solar heating and infrared cooling through the cloud layers. In any case, the deep convective maxima should occur approximately 6-h prior to both the A-train day and night overpasses according to this model. This
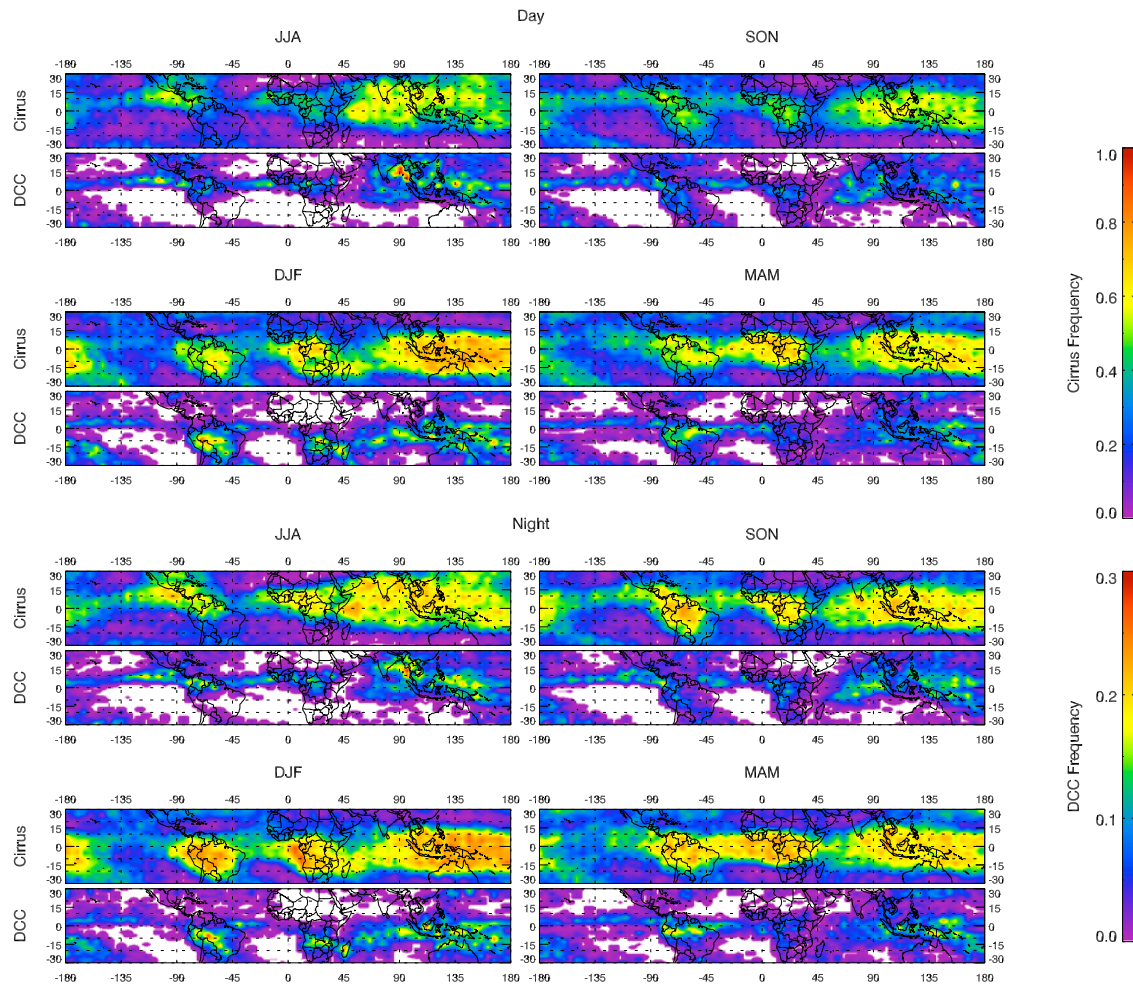
Figure 2. Cirrus and DCC frequency plots as in Figure 1 but broken down into seasons (JJA is June, July, August; SON is September, October, November; DJF is December, January, February; and MAM is March, April, May).

implies that if cirrus clouds are tied to the direct or indirect effects of DCC, there should be observed a diurnal variation of opposite phase over land and ocean [*Tian et al.*, 2004; *Zhang et al.*, 2008]. The diurnal differences in night minus day CALIPSO/CloudSat data for the cirrus and DCC given in Figure 3b, however, indicate that this is not the case. Nowhere in the tropics is there strong evidence for an oceanic day maximum in cirrus, although over land significant nighttime cirrus peaks are apparent (e.g., upper Amazon Basin, equatorial Africa, and Southeast Asia). Actually, there is a tendency for modest nighttime cirrus frequency excesses off the west coast of South America, the central Pacific, and the equatorial Atlantic Ocean, but not in the vast stretch of the western Pacific and Indian Oceans that contains the planet's highest cirrus frequency. The diurnal difference in the frequency of DCC with respect to the standard model of tropical convection is examined below.

[18] Figure 3b indicates a complex pattern of diurnal DCC variability over both land and ocean. Where cirrus clouds are the most abundant over land there are areas of up to about ±5% night/day differences in close proximity to one another, which is also true of the neighboring coastal oceanic areas. In the western Pacific Ocean more diurnal

switches are evident surrounding the major islands. Even in the obvious convective belt of the ITCZ in the Atlantic and Pacific Oceans, diurnal DCC effects seem to alternate between day and night maxima in close proximity. These data indicate a complex variability in convective activity that could be tied to local terrain and weather interactions currently not well understood, which should not be surprising in view of earlier research in regions revealing stark departures from the general diurnal model [e.g., *Nitta and Sekine*, 1994; *Ohsawa et al.*, 2001]. Alternatively, perhaps the 2-year snapshot of measurements shown here suggests that more extended observations of this kind are needed to overcome natural weather and cloud interannual variability.

5. Regional Case Studies

[19] To examine more closely the relationship between deep convection and cirrus clouds along with their diurnal variability, we have chosen 11 separate geographical areas, consisting of at least four connected 2.5° latitude by 5.0° longitude grid boxes, for special analysis that includes day and night cloud height frequencies averaged over a three month period in each year. The locations of the five regions chosen for display here are indicated by the boxes inserted
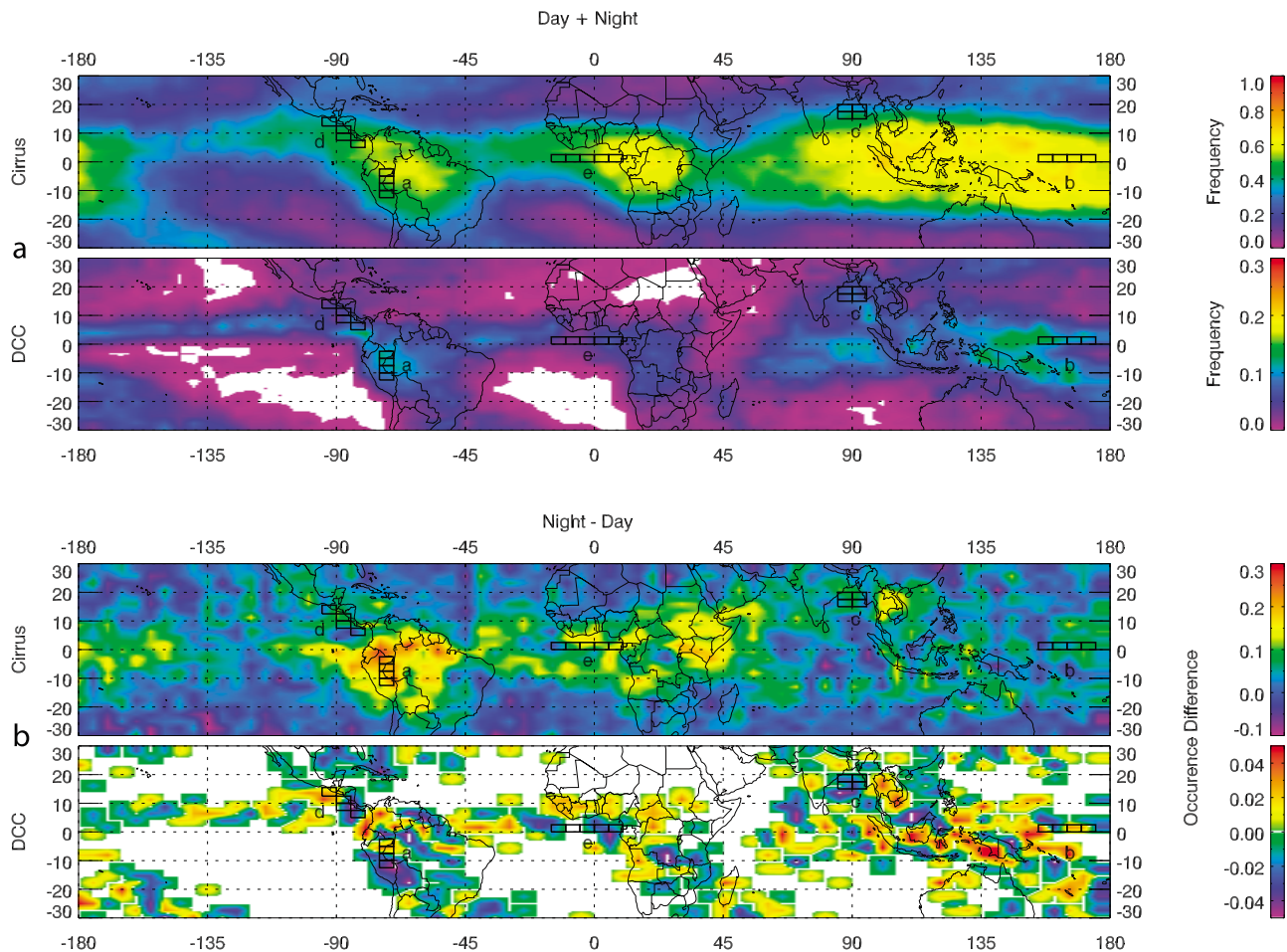
Figure 3. (a) Mean day plus night cirrus cloud (Cirrus) and DCC frequency plots (DCC) compared to (b) the night minus day frequency of occurrences for the same cloud types. In the DCC night-day frequency difference plot, results are only shown for those areas with a frequency >2.5%. Inserted 5.0° longitude by 2.5° latitude boxes show the locations of regional analyses to be discussed later.

in Figure 3. These regions have also generally experienced major field experiments. The sample contains land and ocean areas, most corresponding to regions with both high DCC and cirrus frequencies, such as (for JJA) the west coast of central America and the Bay of Bengal, and (for DJF) the upper Amazon Basin and neighboring coastal waters, the western Pacific, and the eastern Atlantic off west-central Africa. Some areas have been analyzed for both seasons, and subtropical sites were included in the analysis (not shown).

[20] Figure 4 provides representative findings drawn from this sample in terms of 3-month averaged day and night cirrus (solid curve) and DCC (dashed curve) height frequencies. The data are taken from the first year of data collected, but reference is made to the following years findings and Figure 5 is used to illustrate the apparent extent of interannual variability. Turning first to patterns typical of continental areas with high thunderstorm frequencies, Figure 4 (region a) gives results for DJF in the western Amazon Basin, where cirrus are strongly favored at night in both years' data as well as in the 2-year average (Figure 3). DCC in this region do not show a clear diurnal behavior from year to year, but like the cirrus, their cloud top heights tend to be somewhat greater at night. The oceanic site from

the western Pacific Ocean (also DJF) shown in Figure 4 (region b), on the other hand, does not reveal consistent diurnal effects in either cirrus or DCC (see also Figure 3). In Figure 4 (regions c and d) are the results (for JJA) from two coastal areas in the northern hemisphere, namely the Bay of Bengal and the western coast of Central America, respectively. In these regions cirrus frequencies are often greater at night, but can be rather similar also. The DCC frequencies tend to be higher during the day at all altitudes, although the cirrus top heights tend to be higher at night. Finally, the comparison of the 2 years' data across the Gulf of Guinea (region e, for DJF) given in Figure 5 shows some variations from year to year in convective strengths and cirrus amounts, but an increase in cirrus clouds is indicated as the African coastline is approached (from the west). Similar findings are indicated off the western coastlines of central Africa and northern South America, essentially downwind of continental DCC hot spots.

[21] To summarize the findings from these regional studies, the cirrus clouds detected by our CALIPSO/Cloud-Sat algorithm are considerably more frequent over land, particularly during the nighttime overpasses. With the possible exception of some coastal areas, which tend to have more DCC at day than night, no consistent day versus
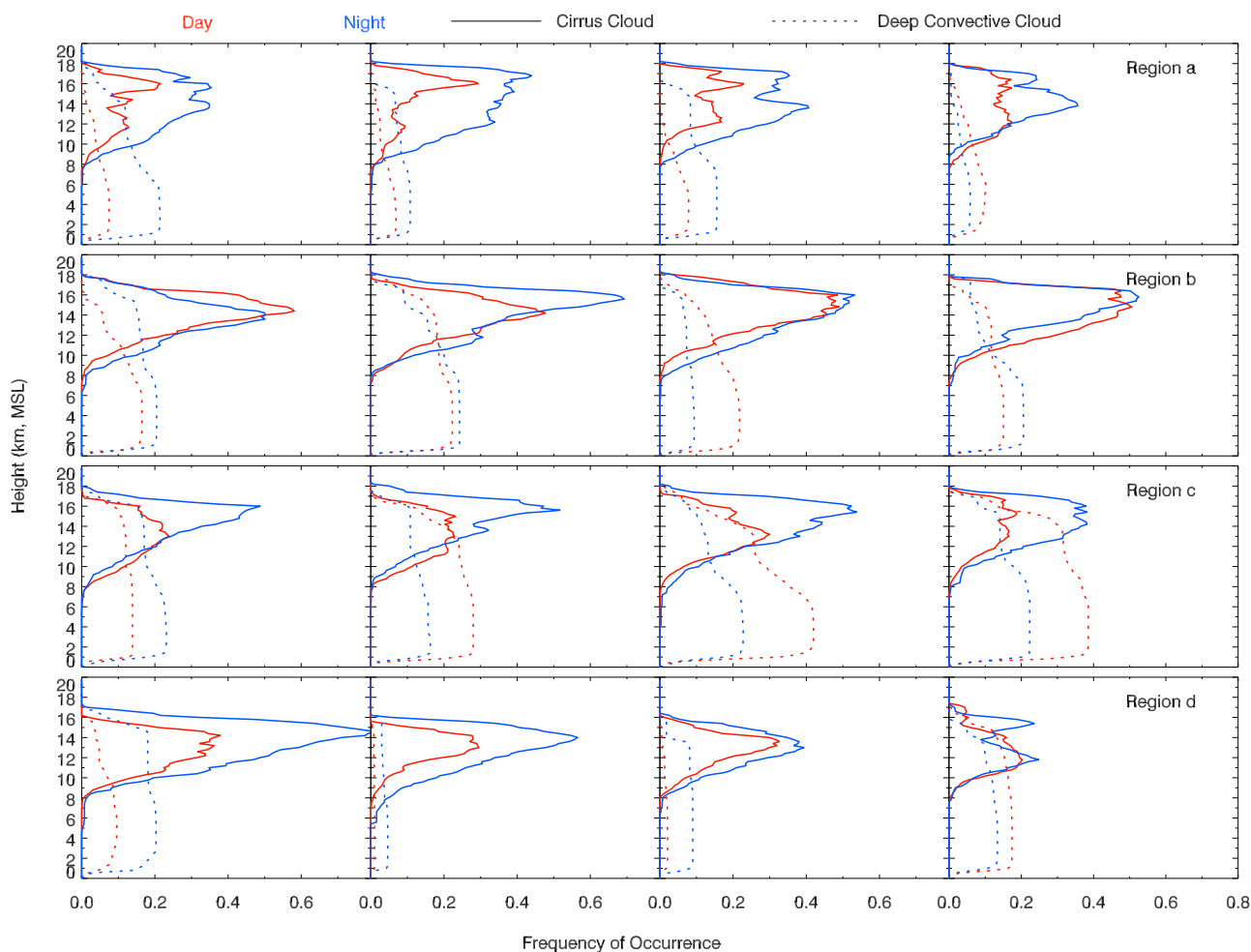
Figure 4. Frequency of occurrence with cloud height of cirrus (solid lines) and DCC (dashed line) for night (blue) and day (red) CALIPSO and CloudSat measurements. Each plot has a letter that identifies its location by the grid boxes shown in Figure 3. The plots here from left to right correspond to grid boxes from top to bottom for region a, from west to east for regions b and e, and from top left to bottom right for regions c and d.

night trend in these deep clouds is observed, however. On the other hand, cirrus cloud top heights are often higher at night by a few hundred meters, warranting further scrutiny. Trends in the frequencies of cirrus clouds off the continental coasts suggest these clouds are consistent with the blow-off from land-based afternoon thunderstorms.

6. Tropical Versus Global Cirrus Properties

[22] In this section the macrophysical and optical properties of tropical cirrus clouds are studied and compared to those of the rest of the globe. The main purpose is to determine if unique conditions apply to tropical cirrus radiative transfer. Considered are the cirrus heights stratified by estimated τ, which impact on the climatic effects of tropical cirrus clouds.

[23] Figure 6 compares the mean night, day, and the night minus day frequencies for the subvisual, thin, and opaque cirrus cloud categories globally. Figure 7 provides the zonal average amounts of these cirrus cloud categories as well as average occurrence of DCC for day and night data. It is clear that subvisual cirrus are primarily a tropical phenom-

enon, although some are found in the midlatitude storm tracks presumably in thin spots and along the edges of visible cirrus [see *Sassen and Cho*, 1992]. The tropics are defined quite well by the band of subvisual cirrus frequencies of $>\sim 5\%$. The thin cirrus category comprises the majority of global cirrus clouds, and is particularly prevalent over northern South America, equatorial Africa, and the western Pacific. Opaque cirrus, on the other hand, are globally widespread, but with a frequency maximum over the East Indian Ocean, Indonesia, and Pacific warm pool regions. The diurnal patterns for the three cirrus cloud optical depth categories are quite different. Whereas subvisual cirrus are favored at night mainly over tropical ocean, thin cirrus clouds are favored at night but over tropical landmasses and island chains. (Note that night/day differences at high latitudes also reflect differences in winter/summer weather patterns.) For thick cirrus clouds, more are generally found during daytime over tropical and midlatitude oceans alike, with some tropical continental regions still showing slight nighttime enhancements. The latitudinal distribution of DCC show maxima of $\sim 5\%$ frequency near the equator, with lesser amounts at midlatitudes.
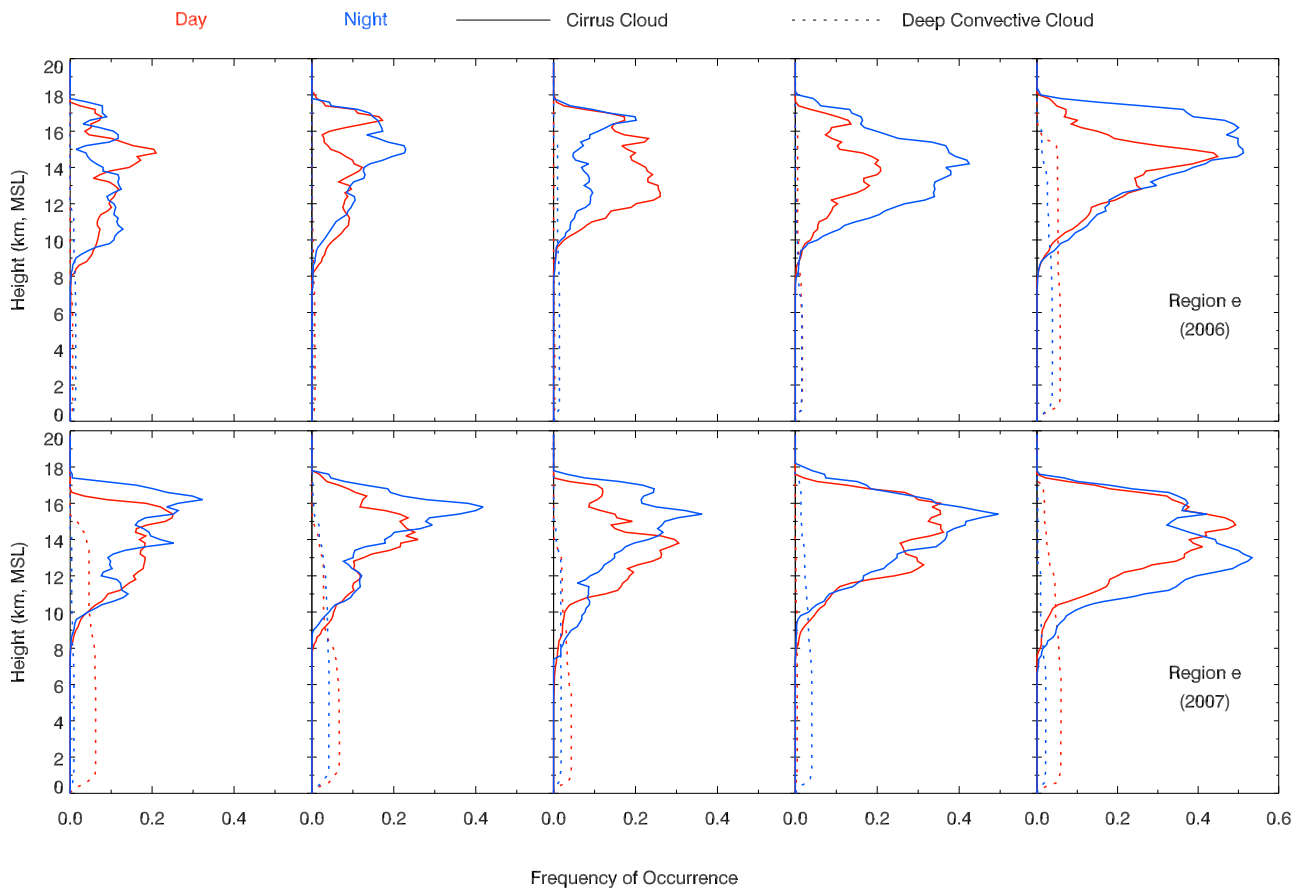
Figure 5. As in Figure 4 but for the region across the Bay of Guinea extending off equatorial Africa shown in Figure 3 (region e, from left to right), for two DJF seasons of data.

[24] With regard to TTL cirrus clouds, these are regarded as occupying the uppermost tropical troposphere, variably as clouds with bases above 14.0 km or 16.0 km above mean sea level (MSL). Shown in Figure 8 are the global mean cirrus cloud frequencies and night minus day differences for these truly high clouds. They are mostly confined to the tropical and subtropical belts, with frequencies of occurrence as high as ~30% and 10%, respectively. It is interesting to note that the >14.0 km MSL cirrus are favored to be detected at night in most regions where they occur the most, but the >16.0 km MSL cirrus do not show a strong tendency for day or night maxima. This is a surprising result
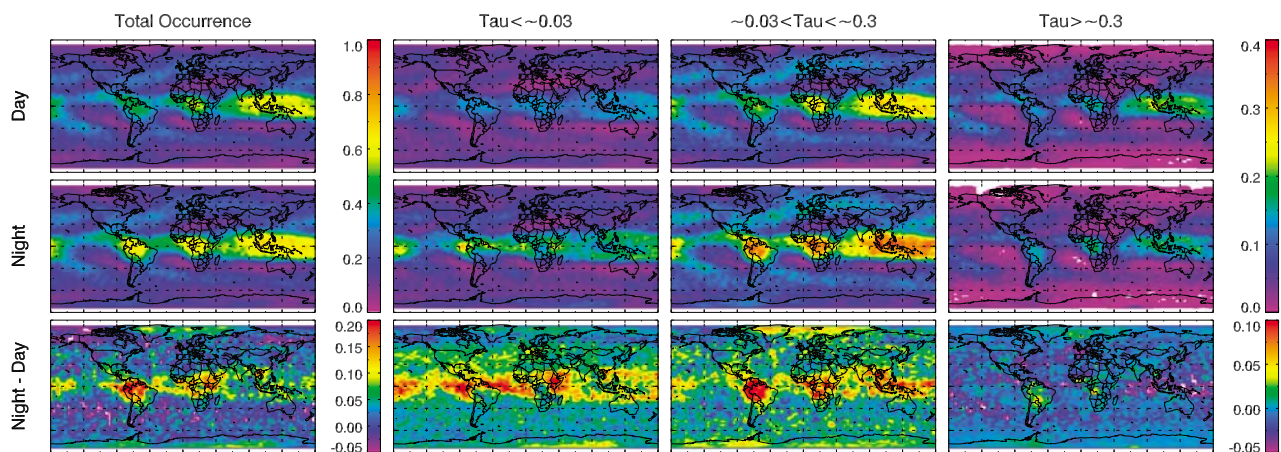
Figure 6. Comparison of day, night, and night minus day cirrus cloud frequencies for the total global occurrence of cirrus, and for those cirrus with estimated optical depths τ <~0.03, ~0.03 to 0.3, and >~0.3, representing subvisual, thin, and opaque cirrus clouds. The calculations assume a lidar ratio of 20 sr.
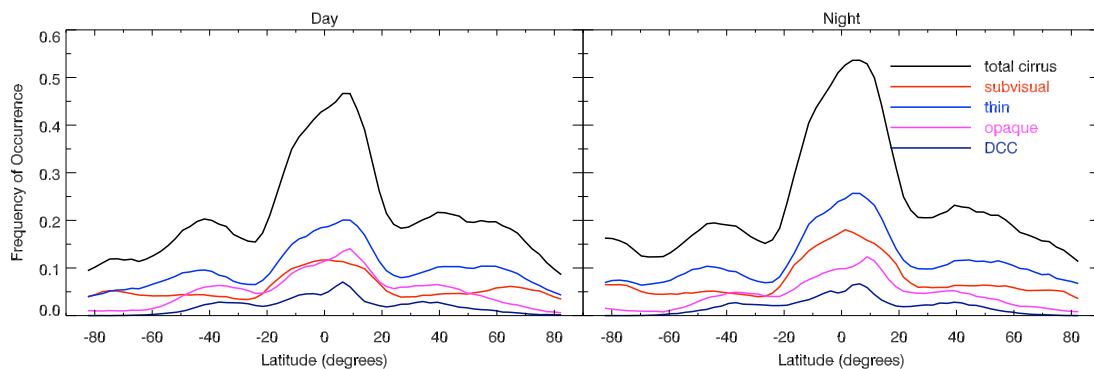
Figure 7. Zonal average occurrence (%) for (left) day and (right) night of global total, subvisual, thin, and opaque cirrus clouds and of DCC.

because it is the latter cirrus that are likely to be the geometrically and optically thinnest clouds in this sample, and so they would be expected to be undersampled during daytime due to possible solar noise effects on CALIOP data collection.

7. Discussion and Conclusions

[25] The evidence from considerable previous research concerning the cause and radiative impact of tropical cirrus clouds, especially in the TTL, is ambiguous. Even the question of how high tropical DCC tops penetrate to, and so create anvil cirrus clouds at the detrainment level, is a matter of debate. While airborne lidar data from the TOGA/CORE project showed frequent cirrus near the tropopause in association with deep convection [*Sassen et al.*, 2000], most research indicates a lower detrainment level, which suggests that TTL cirrus are not directly derived from anvils. Field

projects in various parts of the tropics are typically brief, so it should not be surprising that varied conclusions have been drawn about deep convection and cirrus clouds. A 1-year study using satellite and cloud radar measurements from two islands in the western (Manus) and central (Nauru) equatorial Pacific observed that 47% and 16% of the cirrus, respectively, could be traced back to deep convective activity within a 12-h period [*Mace et al.*, 2006]. This points to the possible major effects of local conditions in the tropical belt on the generation of convection and cirrus clouds, as well as supporting the lack of consistency in findings from earlier field studies.

[26] Alternative theories for tropical cirrus generation that do not involve the direct (anvil) or indirect (cooling above DCC via radiation, pileus-like updrafts, or gravity waves) effects of deep convection rely on planetary-scale waves such as are common at higher latitudes, eastward propagating Kelvin waves in the central Pacific, or tropopause-level
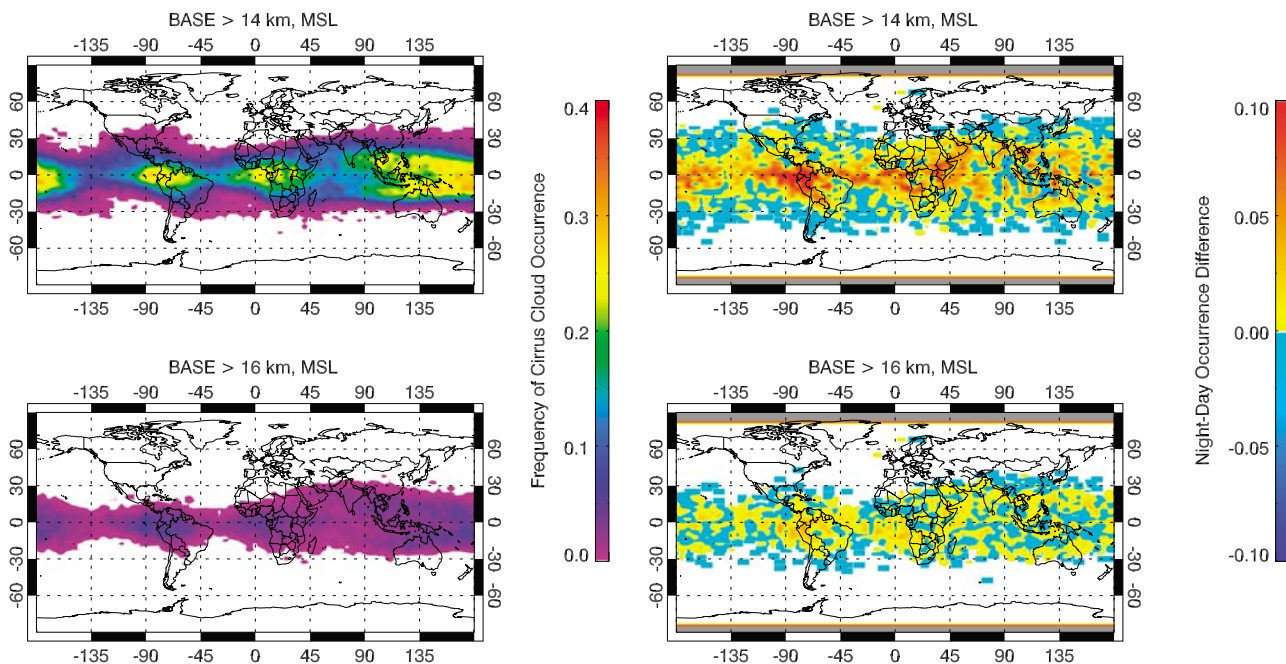
Figure 8. (left) Global frequency of occurrence of all cirrus clouds with cloud base altitudes above 14.0 km MSL and 16.0 km MSL and (right) the corresponding night minus day differences, approximating the presence of tropical tropopause layer (TTL) cirrus clouds.

radiative effects. The processes involved in cirrus formation are important because they modulate the resulting micro-physical/radiative effects of the layer [*Sassen*, 2002]. Normally, cirrus have significant shortwave (SW) and long-wave (LW) cloud radiative forcing, but in combination they are generally believed to lead to warming, greenhouse effect. Accepting that the optical depth upper limit for cirrus is in the 3.0–4.0 range, both the SW sunlight reflected by cirrus and the LW terrestrial radiation trapped by cirrus depend on τ, with the latter also strongly depending on the cloud top temperature and the temperature of the surface or clouds below. Thus the radiative transfer situation in the tropics with coexisting convective and cirrus clouds is complex, being strongly influenced by the vertical structure of all clouds present. It is also important to note that cirrus cloud particle sizes tend to decrease with decreasing temperature, and in the frigid tropical upper troposphere it is possible that ice crystal sizes are small enough to be inefficient absorbers of LW radiation, as some evidence suggests [*Platt et al.*, 1998], leading to a potential reversal of the usual greenhouse warming effect [e.g., see *Räisänen et al.*, 2006].

[27] From the orbiting range-resolved remote sensing data presented here, it is clear that tropical DCC are embedded in the centers of those expansive regions over land and water that contain the planets' most abundant cirrus clouds: where cirrus are uncommon ($<\sim$10% mean frequency), DCC are essentially absent. For example, from Figure 1 it can be seen that a $\sim$5% DCC frequency contour would correspond well to the area contained within the core $\sim$50% cirrus cloud frequency. This implies that cirrus cloud formation in the tropics is generally tied to the direct and/or indirect effects of deep convection. Although considerable variability exists in the indicated diurnal behavior of DCC, the cirrus, on the other hand, display a strong nocturnal frequency increase particularly over land of up to $\sim$30% (see Figure 3). Some ocean areas, particularly along the coasts of landmasses displaying relatively frequent convection, and in the central Pacific area, also display a nighttime preference for cirrus. Taking a more global view and stratifying the data according to estimated cirrus τ (Figure 6), we note that the frequencies of subvisual cirrus clouds are highest at night and in the tropics, especially over ocean. (However, land areas like eastern central Africa have a strong nocturnal preference for these clouds as well, which is inconsistent with scattered solar noise effects on CALIPSO cirrus cloud detection.) Thin cirrus clouds are also more abundant at night, but in this case mainly over land, not water. These two results could be consistent with a late afternoon–evening maximum in land convection [*Liu and Zipser*, 2008], assuming that near coastal regions the cirrus decay and become optically thinner with time as they drift away from their source regions. (But this does not account for the strong nighttime cirrus increase over the central Pacific area.) As for opaque cirrus, these show some preference for daytime over water, which could be consistent for cirrus generated in association with early morning marine convection, while a weakened nocturnal increase remains over land.

[28] To account for these temporal patterns in cirrus and DCC clouds, there are two possibilities: either the findings are real and somehow related to the timing of deep con-

vection (relative to the twice-daily satellite observations), or the results are merely due to solar noise effects in CALIOP data. Although signal noise effects will affect cloud detection, the observed patterns in cirrus cloud occurrence differences are simply too large to be explained away by noise. Ship-borne lidar measurements in the Pacific warm pool have noted a tendency for upper tropospheric cirrus layers to descend and disappear during the day [*Iwasaki et al.*, 2004]. Recall also that the highest TTL cirrus clouds studied here do not display a noticeable diurnal variation. Thus we believe that the diurnal cirrus patterns mostly reflect real cloud processes, which must be driven by tropical convection to a large degree to explain the similarity in the cirrus and DCC distributions. DCC are central to the tropical cirrus cloud regions, from which the cirrus may spread by advection and eventually decay. TTL cirrus may not adhere to this pattern, but cirrus directly generated through spreading anvils, and indirectly by convectively generated gravity waves, etc, will. What remains to be determined is the longevity of such wave disturbances (i.e., the distances over which the waves will act to form new cirrus), and the longevity of the cirrus layers that formed from DCC anvils and are transported by horizontal winds. Cloud models should help to answer these important questions in light of these new observations.

[29] Of course, there are interesting exceptions to these general patterns of tropical cloud behaviors revealed by CALIPSO and CloudSat, which should be pursued in further research. For example, eastern equatorial Africa and the adjacent Indian Ocean, and the central Pacific warm pool, have unusual behaviors, i.e., considerable subvisual cirrus and a strong JJA cirrus hot spot, and a nocturnal cirrus maximum in the middle of an ocean, respectively.

[30] To better examine the issue of diurnal variability in cirrus clouds and DCC and their characteristics in the tropics, it may be that, in view of interannual weather variability and the relatively small cloud volumes actually probed by current spaceborne active remote sensors, more extended data is needed. It should also be reiterated that the timing of the twice-daily local A-train overpasses may not be in sync with actual DCC diurnal variations: although the night overpasses appear to correspond to the presence of increased deep convection over ocean, the daytime data are obtained just prior to the evening DCC maximum according to TRMM data [*Liu and Zipser*, 2008]. Thus, we welcome the extended lifetime provided by NASA to these missions, and look forward to the potential in the future of new and enhanced, perhaps scanning lidars and cloud radars in Earth orbit.

References

Boehm, H. P., and J. Verlinde (2000), Stratospheric influence on upper tropospheric tropical clouds, *Geophys. Res. Lett.*, *27*, 3209–3212, doi:10.1029/2000GL011678.

Bourassa, A. E., D. A. Degenstein, and E. J. Llewellyn (2005), Climatology of subvisual cirrus clouds as seen by OSIRIS on Odin, *Adv. Space Sci.*, *36*, 807–812, doi:10.1016/j.asr.2005.05.045.

Cadet, B., L. Goldfarb, D. Faduilhe, S. Baldy, V. Giraud, P. Keckhut, and A. Réchou (2003), A sub-tropical cirrus clouds climatology from Reunion Island (21°S, 55°W) lidar data set, *Geophys. Res. Lett.*, *30*(3), 1130, doi:10.1029/2002GL016342.

Chen, W. N., C. W. Chiang, and J. B. Nee (2002), Lidar ratio and depolarization ratio for cirrus clouds, *Appl. Opt.*, *41*, 6470–6497, doi:10.1364/AO.41.006470.

Comstock, J. M., T. Ackerman, and G. G. Mace (2002), Ground-based lidar and radar remote sensing of tropical cirrus clouds at Nauru Island: Cloud statistics and radiative impacts, *J. Geophys. Res.*, *107*(D23), 4714, doi:10.1029/2002JD002203.

Dessler, A. E., S. P. Palm, W. D. Hart, and J. D. Spinhirne (2006), Tropopause-level thin cirrus coverage revealed by ICESat/Geoscience Laser Altimeter System, *J. Geophys. Res.*, *111*, D08203, doi:10.1029/2005JD006586.

Garrett, T. J., et al. (2006), Convective formation of pileus cloud near the tropopause, *Atmos. Chem. Phys.*, *6*, 1185–1200.

Gray, W. M., and R. W. Jacobson Jr. (1977), Diurnal variation of deep cumulus convection, *Mon. Weather Rev.*, *105*, 1171–1188, doi:10.1175/1520-0493(1977)105<1171:DVODCC>2.0.CO;2.

Heymsfield, A. J. (1986), Ice particles observed in a cirriform cloud at −83° and implications for polar stratospheric cloud, *J. Atmos. Sci.*, *43*, 851–855, doi:10.1175/1520-0469(1986)043<0851:IPOIAC>2.0.CO;2.

Iwasaki, S. Y., et al. (2004), Subvisual cirrus cloud observations using a 1065-nm lidar, a 95 GHz cloud radar, and radiosondes in the warm pool region, *Geophys. Res. Lett.*, *31*, L09103, doi:10.1029/2003GL019377.

Jensen, E. J., O. B. Toon, H. B. Selkirk, J. D. Spinhirne, and M. R. Schoeberl (1996), On the formation and persistence of subvisible cirrus clouds near the tropical tropopause, *J. Geophys. Res.*, *101*, 21,361–21,375.

Liu, C., and E. J. Zipser (2008), Diurnal cycles of precipitation, clouds, and lightning in the tropics from 9 years of TRMM observations, *Geophys. Res. Lett.*, *35*, L04819, doi:10.1029/2007GL032437.

Mace, G. G., M. Deng, B. Soden, and E. Zipser (2006), Association of tropical cirrus in the 10–15-km layer with deep convective sources: An observational study combining millimeter radar data and satellite-derived trajectories, *J. Atmos. Sci.*, *63*, 480–503, doi:10.1175/JAS3627.1.

Matrosov, S. Y. (2007), Potential for attenuation-based estimations of rainfall rate from CloudSat, *Geophys. Res. Lett.*, *34*, L05817, doi:10.1029/2006GL029161.

McFarquhar, G. M., A. J. Heymsfield, J. Spinhirne, and B. Hart (2000), Thin and subvisual tropopause tropical cirrus: Observations and radiative impacts, *J. Atmos. Sci.*, *57*, 1841–1853, doi:10.1175/1520-0469(2000)057<1841:TASTTC>2.0.CO;2.

Nitta, T., and S. Sekine (1994), Diurnal variation of convective activity over the tropical western Pacific, *J. Meteorol. Soc. Jpn.*, *72*, 627–641.

Ohsawa, T., H. Ueda, T. Hayashi, A. Watanabe, and J. Matsumoto (2001), Diurnal variations of convective activity and rainfall in tropical Asia, *J. Meteorol. Soc. Jpn.*, *79*, 333–352, doi:10.2151/jmsj.79.333.

Platt, C. M. R., S. A. Young, P. J. Manson, G. R. Patterson, S. C. Marsden, R. T. Austin, and J. Churnside (1998), The optical properties of equatorial cirrus from observations in the ARM Pilot Radiation Observation Experiment, *J. Atmos. Sci.*, *55*, 1977–1996, doi:10.1175/1520-0469(1998)055<1977:TOPOEC>2.0.CO;2.

Platt, C. M. R., R. T. Austin, S. A. Young, and G. R. Patterson (2002), LIRAD observations of tropical cirrus clouds in MCTEX. Part I: Optical properties and detection of small particles in cold cirrus, *J. Atmos. Sci.*, *59*, 3145–3162, doi:10.1175/1520-0469(2002)059<3145:LOOTCC>2.0.CO;2.

Prabhakara, C., D. P. Kratz, J.-M. Yoo, G. Dalu, and A. Vernekar (1993), Optically thin cirrus clouds: Radiative impact on the warm pool, *J. Quant. Spectrosc. Radiat. Transfer*, *49*, 467–483, doi:10.1016/0022-4073(93)90061-L.

Räisänen, P., A. Bogdan, K. Sassen, M. Kulmala, and M. J. Molina (2006), Impact of H_2SO_4/H_2O coating and ice crystal size on radiative properties of sub-visible cirrus, *Atmos. Chem. Phys.*, *6*, 4659–4667.

Rosenfield, J. E., D. B. Considine, M. R. Schoeberl, and E. V. Browell (1998), The impact of subvisual cirrus clouds near the tropical tropopause on stratospheric water vapor, *Geophys. Res. Lett.*, *25*, 1883–1886, doi:10.1029/98GL01294.

Sassen, K. (2002), Cirrus clouds: A modern perspective, in *Cirrus*, edited by D. Lynch et al., pp. 11–40, Oxford Univ. Press, Oxford, U. K.

Sassen, K., and B. S. Cho (1992), Subvisual/thin cirrus dataset for satellite verification and climatological research, *J. Appl. Meteorol.*, *31*, 1275–1285, doi:10.1175/1520-0450(1992)031<1275:STCLDF>2.0.CO;2.

Sassen, K., and Z. Wang (2008), Classifying clouds around the globe with the CloudSat radar: 1-year of results, *Geophys. Res. Lett.*, *35*, L04805, doi:10.1029/2007GL032591.

Sassen, K., R. P. Benson, and J. D. Spinhirne (2000), Tropical cirrus cloud properties from TOGA/COARE airborne polarization lidar, *Geophys. Res. Lett.*, *27*, 673–676, doi:10.1029/1999GL010946.

Sassen, K., S. Matrosov, and J. Campbell (2007), CloudSat spaceborne 94 GHz radar bright bands in the melting layer: An attenuation-driven upside-down lidar analog, *Geophys. Res. Lett.*, *34*, L16818, doi:10.1029/2007GL030291.

Sassen, K., Z. Wang, and D. Liu (2008), Global distribution of cirrus clouds from CloudSat/Cloud-Aerosol Lidar and Infrared Pathfinder Satellite Observations (CALIPSO) measurements, *J. Geophys. Res.*, *113*, D00A12, doi:10.1029/2008JD009972.

Stephens, G. L., et al. (2002), The CloudSat mission and the A-train: A new dimension of space-based observations of clouds and precipitation, *Bull. Am. Meteorol. Soc.*, *83*, 1771–1790, doi:10.1175/BAMS-83-12-1771.

Tian, B., et al. (2004), Diurnal cycle of convection, clouds, and water vapor in the tropical upper troposphere: Satellites versus a general circulation model, *J. Geophys. Res.*, *109*, D10101, doi:10.1029/2003JD004117.

Wang, P. H., P. Minnis, M. P. McCormick, G. S. Kent, and K. M. Skeens (1996), A 6-year climatology of cloud occurrence frequency from Stratospheric Aerosol and Gas Experiment II observations (1985–1990), *J. Geophys. Res.*, *101*, 29,407–29,430, doi:10.1029/96JD01780.

Winker, D. M., and C. R. Trepte (1998), Laminar cirrus observed near the tropical tropopause by LITE, *Geophys. Res. Lett.*, *25*, 3351–3354, doi:10.1029/98GL01292.

Winker, D. M., W. H. Hunt, and M. J. McGill (2007), Initial performance assessment of CALIOP, *Geophys. Res. Lett.*, *34*, L19803, doi:10.1029/2007GL030135.

Yang, G.-Y., and J. Slingo (2001), The diurnal cycle in the tropics, *Mon. Weather Rev.*, *129*, 784–801, doi:10.1175/1520-0493(2001)129<0784:TDCITT>2.0.CO;2.

Zhang, Y., S. A. Klein, C. Liu, B. Tian, R. T. Marchand, J. M. Haynes, R. B. McCoy, Y. Zhang, and T. P. Ackerman (2008), On the diurnal cycle of deep convection, high-level cloud, and upper tropospheric water vapor in the Multiscale Modeling Framework, *J. Geophys. Res.*, *113*, D16105, doi:10.1029/2008JD009905.

————————

D. Liu and Z. Wang, Atmospheric Science Department, University of Wyoming, Laramie, WY 82071, USA.

K. Sassen, Geophysical Institute, University of Alaska Fairbanks, Fairbanks, AK 99775, USA. (ksassen@gi.alaska.edu)